

# Magnetic properties of Ising thin-films with cubic lattices

Y. Laosiritaworn<sup>†</sup>, J. Poulter<sup>‡</sup> and J.B. Staunton<sup>†</sup>

<sup>†</sup> *Department of Physics, University of Warwick,  
Coventry CV4 7AL United Kingdom and*

<sup>‡</sup> *Department of Mathematics, Faculty of Science,  
Mahidol University, Bangkok 10400, Thailand.*

## Abstract

We have used Monte Carlo simulations to observe the magnetic behaviour of Ising thin-films with cubic lattice structures as a function of temperature and thickness especially in the critical region. The fourth order Binder cumulant is used to extract critical temperatures, and an extension of finite size scaling theory for reduced geometry is derived to calculate the critical exponents. Magnetisation and magnetic susceptibility per spin in each layer are also investigated. In addition, mean-field calculations are also performed for comparison. We find that the magnetic behaviour changes from two dimensional to three dimensional character with increasing thickness of the film. The crossover of the critical temperature from a two dimensional to a bulk value is also observed with both the Monte Carlo simulations and the mean-field analysis. Nevertheless, the simulations have shown that the critical exponents only vary a little from their two dimensional values. In particular, the results for films with up to eight layers provide a strong indication of two dimensional universality.

PACS numbers: 64.60.Fr, 75.40.Cx, 75.40.Mg, 75.70.Ak

## I. INTRODUCTION

Studies of the dimensional crossover of magnetic properties from two dimensional ( $2d$ ) to three dimensional ( $3d$ ) character in magnetic multi-layers have currently attracted much interest. An understanding of the physical properties of solids as the dimensionality is reduced is of both technological and fundamental importance [1, 2]. In particular, studies of ultrathin magnetic films have revealed a number of novel phenomena that would not have been expected in either  $2d$  or  $3d$  systems. Of particular interest is the critical behaviour of magnetic thin-films, for which the dimensionality  $d$  is not well established. It is interesting to consider how magnetic properties such as the magnetisation  $m$ , magnetic susceptibility  $\chi$  and critical temperature  $T_C$  are affected by the finiteness of the system in the direction perpendicular to the film.

From both theoretical and experimental studies, the critical temperature  $T_C$  is found to increase with film thickness. Nevertheless, how the thickness  $l$  of the film relates to the dimensional crossover of other magnetic critical properties from  $2d$  to bulk  $3d$  is not fully understood. Most studies imply that magnetic films belong to a  $2d$  universality class regardless of the thickness. This is commonly understood to be a consequence of the finiteness of the films along the out-of-plane direction. Close to the phase transition point (critical temperature  $T_C$ ) the correlation length  $\xi$  is constrained by thickness and allowed to expand only in the in-plane direction. This is certainly a  $2d$ -like phenomenon. However, well-known experimental studies of thin-films of nickel [3] have shown contrary evidence where a dimensional crossover of the critical exponent  $\beta$  from  $2d$  to  $3d$  has been found. Hence, to clarify this discrepancy, we consider the use of Ising thin-films to study such a phenomenon in cubic lattices, that is simple cubic (sc), body centred cubic (bcc) and face centred cubic (fcc).

The Ising model represents a ferromagnet with infinite uniaxial anisotropy. It is useful because strong magnetic anisotropies are common in ultrathin ferromagnetic films and monolayers. In addition, it turns out that  $2d$  anisotropic Heisenberg systems become Ising-like near  $T_C$ . This was shown by Binder and Hohenberg [4] using Monte Carlo simulations and has been proven rigorously by Bander and Mills [5] using renormalisation group analysis. Also, from the experimental point of view, experiments on nickel [3] and iron thin-films [6] have shown  $2d$  results in agreement with Ising  $2d$  critical exponents. These all suggest that the Ising model is a handy tool to study magnetic thin-films.

Previous studies of Ising thin-films have been by means of the high temperature expansion [7, 8], renormalisation group [9], variational cumulant expansion (VCE) [10] and Monte Carlo [11, 12] methods. However, most of them have concentrated on the study of the critical temperature and shift exponent in the sc lattice. Few have investigated the effective critical exponents in order to determine how they vary as a function of temperature away from  $T_C$ . As far as we are aware, nothing exists in the literature reporting the investigation of critical exponents as a function of thickness at the critical point. This is mainly due to a presumption that the films are of the  $2d$  class as well as difficulties in the analysis due to finite size effects. Hence, in this study, we aim to give a more complete picture of the magnetic phase transition in thin-films especially at the critical point. We have investigated how the magnetic properties vary as a function of temperature and thickness by means of Monte Carlo simulations and mean-field theory. We have also calculated the critical temperature and investigated its convergence to the bulk limit. Most crucially, we have developed an extension to finite size scaling analysis to observe how the critical exponents vary as a function of thickness. In outline, we firstly describe the numerical calculations and the methods we have used. Secondly, we show the evolution of the magnetic properties as a function of temperature and thickness. Then, we report the critical properties of thin-films in terms of critical temperatures and exponents. Finally, we discuss our results and compare the characteristic critical exponents with those found in experiments.

## II. METHODOLOGY

The starting point for the study is the nearest neighbor Ising hamiltonian

$$H = -J \sum_{\langle ij \rangle} S_i S_j, \quad (1)$$

where the spin  $S_i$  takes on the values  $\pm 1$  and the sum includes only first nearest-neighbor (1nn) pairs. Helical and free boundary conditions are used in our simulations using this hamiltonian for the in-plane and out-of-plane directions respectively. We use units of  $J/k_B$  and  $J$  for temperature and energies respectively with the magnetisation per spin defined as  $m = \frac{1}{N} \sum S_i$  where  $N$  is total number of spins.

The simulations are carried out for sc, fcc and bcc films of size  $N = L \times L \times l$  where  $L \times L$  represents the number of sites in each layer of the film and  $l$  is the number of layers in the film i.e. its thickness. We vary  $L$  from 64 to 128 (in steps of 8) with  $l$  ranging from a monolayer (bilayer for bcc films) to 20 layers. The spin configurations of the films are updated using the highly efficient Wolff algorithm [13] to minimise the effect from statistical errors arising from correlation time [14, 15]. The random number generator (drand48) is chosen carefully [16, 17, 18] and we ensure that different seed numbers have no significant effect on the results. For each simulation, roughly  $3,000 \times N$  spins are updated before the system is deemed to have reached equilibrium. From this point,  $5 \times 10^5$  independent configurations are used to calculate the expectation of magnetisation per spin  $\langle m \rangle = \frac{1}{t_{\max}} \sum_i^{t_{\max}} |m_i|$ , where  $t_{\max}$  is total number of measured configurations, and the magnetic susceptibility  $\chi = \beta N (\langle m^2 \rangle - \langle |m| \rangle^2)$  ( $\beta \equiv J/k_B T$ ). In a similar fashion, the layer-dependence of these magnetic properties,  $m_k$  and  $\chi_k$ , where  $k$  is a layer index, are calculated in order to observe the surface effects upon the magnetic properties. For the investigation of the critical behaviour of the films, we locate the critical temperatures ( $T_C$ ) via the fourth order cumulant  $U_L$  [19]

$$U_L = 1 - \frac{1}{3} \frac{\langle m^4 \rangle}{\langle m^2 \rangle^2}. \quad (2)$$

At  $T = T_C$ ,  $U_L$  should be independent of  $L$ , i.e. for differing sizes  $L, L'$   $(U_{L'}/U_L)_{T=T_C} = 1$ . Owing to finite size effects, we need to plot  $T_C(b)$  ( $L = bL'$ ) against  $(\ln b)^{-1}$ , and extrapolate the results to the infinite limit i.e.  $(\ln b)^{-1} \rightarrow 0$  [19]. To maximise the efficiency of this  $T_C$  calculation, for each thickness, we perform a single long simulation at a temperature  $T_0$  and use the histogram method [20, 21] to extrapolate  $U_L$  to a temperature nearby in order to find the cumulant crossing point. This temperature is chosen from the temperature at the peak of the magnetic susceptibility curve for the  $L = 128$  system, and then around 1 to 4 million spin configurations are used to create the histograms. To exclude those data obtained from temperatures too far from the simulated temperature  $T_0$ , the range of extrapolation  $|T - T_0|$  is restricted by the criterion  $|U(T) - U(T_0)| \leq \sigma_E$  [22] where  $U \equiv \langle E \rangle$ , the average of the energy, and  $\sigma_E$  is a standard deviation of  $E$  at  $T_0$ .

The next step is to extract the critical exponents from our finite size results. To do this we have developed a finite size scaling method appropriate for films in which  $l/L \ll 1$ . The purpose is to find how magnetic properties  $m$  and  $\chi$  scale with the size  $L$  and  $l$  of the systems. The basic finite size scaling ansatz (e.g. [23, 24, 25, 26, 27, 28]) rests on an assumption that only a single correlation length  $\xi$  is needed to describe the critical properties of thin-films. As detailed in Appendix A this gives the following general form for how the magnetisation and susceptibility scale with  $L$

$$\begin{aligned} \langle m(T, l) \rangle &= L^{-\beta/\nu} \tilde{m}(L^{1/\nu} t, l), \\ \chi(T, l) &= L^{(\gamma/\nu)'} \tilde{\chi}(L^{1/\nu} t, l), \end{aligned} \quad (3)$$

where  $(\gamma/\nu)' = \gamma/\nu + 2 - d$ .  $\gamma$ ,  $\beta$  and  $\nu$  are the critical exponents associated with  $\chi$ ,  $m$  and  $\xi$  respectively,  $\tilde{\chi}$  and  $\tilde{m}$  are scaling functions for a given  $l$  and  $t = 1 - \frac{T}{T_C}$  is the reduced temperature. These scaling functions for a range of  $L$  should collapse onto a single curve with the correct critical temperature and exponents. The exponent  $1/\nu$  can be extracted from the derivative of the cumulant with respect to  $L$  at  $T_C$

owing to its variation with system size as  $L^{1/\nu}$  [19]. Since we have assumed that there is a single  $\xi \propto t^{-\nu}$  a single  $\nu$  is to be expected. Note that if equations (3) correctly encapsulate the nature of magnetic critical behaviour in films, we can extract the exponents  $\beta/\nu$  and  $(\gamma/\nu)'$  by plotting  $\log m$  and  $\log \chi$  against  $\log L$  at  $T_C$ . Before this can be done with confidence it is necessary to demonstrate the validity of the assumption of a single correlation length and thus the form of equations (3). This can be done by establishing the following :-

1. According to eqn. (3), at  $T_C$ , if we plot  $\log \chi (m)$  against  $\log L$  we should get a straight line.
2. We should find that the sum of  $(\gamma/\nu)' + 2(\beta/\nu)$  is always equal to 2. This again can be derived using the assumption of a single correlation length and  $\gamma/\nu + 2\beta/\nu = d$  [29] i.e.

$$\left(\frac{\gamma}{\nu}\right)' + 2\frac{\beta}{\nu} = \frac{\gamma}{\nu} + 2 - d + 2\frac{\beta}{\nu} = 2, \quad (4)$$

3. The clearest demonstration comes from a direct examination of the scaling functions themselves, eqn. (3). With correct exponents in the critical region, a scaling function for any  $L$  but a particular  $l$  should collapse onto a single curve. This will also confirm the reliability of the critical exponents extracted from our simulations

### III. RESULTS AND DISCUSSION

#### A. Magnetisation and Magnetic Susceptibility

The magnetisation  $m$  and susceptibility  $\chi$  profiles for various film thicknesses  $l$  and system sizes  $L$  are obtained. The crossover of magnetic behaviour from  $2d$ -like for the monolayer (bilayer in bcc) to  $3d$ -like for films with 20 or more layers is found. For example, Fig. 1a,b shows the magnetic phase transition for a system of  $128 \times 128 \times l$  spins. The transition point moves from  $2d$  to  $3d$  values with increasing film thickness. The layer resolution of these magnetic properties is also investigated. The influence of the surface on the magnetic properties can also be seen. For instance, Fig. 1c and d show the layer-dependence of  $m_k$  and  $\chi_k$  for the  $128 \times 128 \times 10$  system. The surface layer has the lowest magnetisation magnitude, whilst the magnetisation per site increases towards the interior of the films. Similarly, for  $\chi$ , representing the fluctuation of  $m$ , the strongest magnitude is for the innermost layer and the weakest is at the surface. The  $k^{th}$  and  $(l - k)^{th}$  layers have the same magnetic properties owing to the spatial symmetry and the isotropy of  $J$ .

The layer variation of the magnetic properties can be explained in terms of finiteness of the thin-films along the  $z$  direction together with the Monte Carlo updating algorithm. In a simulation run, once a seed spin is chosen in order to select a group of spins to be updated with the Wolff algorithm, it will have a greater chance of aligning those neighboring spins which are located towards the interior of the films rather than those towards the surface. Consider the probability for a site getting updated:

$$D(i, j, k) = \frac{1}{M} \sum_{n=1}^M s'(i, j, k), \quad (5)$$

where  $s'(i, j, k)$  is the number of times the site at location  $(i, j, k)$  is in a Wolff update, and  $M$  is the total number of clusters forming (flipping) in a simulation. Our simulations show that, in the ferromagnetic phase,  $D$  at the surface layers always has the lowest magnitude, except, at very low  $T$  where the chance of a site getting updated is very high and the same anywhere. Thus, this implies that once a cluster of spins is formed, the group has its spins preferentially located in the inner layers rather than near the surface layers. When the group is flipped, the inner layer will always have the high magnetisation magnitude, but at the surface layers, there will be more un-flipped spins behaving as a buffer which results in smaller

magnetisation magnitude. Similarly, for the susceptibility, the buffer in the surface layers helps to reduce the magnetic fluctuation leading to a smaller susceptibility than for the inner layers.

We find the same qualitative trends by using a mean-field approximation (see appendix B). The evolution of the magnetic properties from  $2d$ - to  $3d$ -like is again found e.g. for sc films in Fig. 2a,b. The layer-dependence of magnetic properties is also evident. As expected, the magnetisation per site is smallest on the surface layer and highest on the innermost as can be seen, for example, in Fig. 2c,d which show results for a 10-layered Ising sc film.

## B. Critical Temperatures and Shift Exponents

We calculate the critical temperatures of the films from our Monte Carlo simulations using the cumulant method. The results are summarised in Table I. We find a change from  $2d$  to bulk values as  $l$  is increased. Fig. 3a shows evidence of such a dimensional crossover for the Ising thin-films. Both our  $2d$  and bulk results agree very well with the exact Ising  $2d$  results and previous Ising  $3d$  studies [21, 30]. As the number of layers is increased, the critical temperature moves towards the  $3d$  value owing to the increase of the average exchange interaction energy. On similar grounds, for  $l \geq 4$ , we find  $T_C^{\text{sc}}(l) < T_C^{\text{bcc}}(l) < T_C^{\text{fcc}}(l)$ . The mean-field theory calculations show the same qualitative trends (Fig. 3b) but, as expected, the estimated  $T_C$ 's are consistently higher than those from the Monte Carlo work. Moreover an analytic expression for  $T_C$  as a function of film thickness has been made on the basis of a mean-field  $T_C$  examination [31]. This is given as,

$$T_C(l) = T_C(\infty) \frac{z_0 + 2z_1 \cos(\pi/(l+1))}{z_0 + 2z_1}, \quad (6)$$

where  $z_0$  and  $z_1$  are number of nearest neighbors in the same plane and its adjacent plane respectively. We find our mean-field results to comply with this expression. A summary of results for  $T_C$  from both Monte Carlo and mean-field calculations is presented in Table I and Fig. 3.

It is revealing to examine the evolution of the thin-films' critical temperatures from the monolayer to bulk  $3d$  limit in terms of a power law

$$1 - \frac{T_C(l)}{T_C(\infty)} \propto l^{-\lambda}, \quad (7)$$

Here  $T_C(\infty)$  is the bulk critical temperature and the shift exponent  $\lambda$  has a value between 1.0 and 2.0 depending on the spin model used and the type of calculation. For thick films  $\lambda$  is expected to be  $1/\nu^{3d}$  [27]. A better fit for films of a range of thicknesses  $l$  is given by [32] and has the form

$$\frac{1}{T_C(l)} = \frac{1}{T_C(\infty)} \left[ 1 + \left( \frac{l_0}{l-l'} \right)^{\lambda'} \right], \quad (8)$$

where  $l_0$ ,  $l'$  and  $\lambda'$  are all adjustable parameters. Similarly,  $\lambda'$  should tend to  $1/\nu^{3d}$  as  $l \rightarrow \infty$ .

We use eqn. (8) to fit the  $T_C(l)$ 's arising from our Monte Carlo calculations. If it turns out that our  $T_C(l)$ 's are accurate and that the fit is a useful one, we should find  $T_C(\infty)$  in agreement with the  $T_C^{\text{bulk}}$  we calculate separately. Results of the fit are shown in Table II, and there is less than a 1 percentage difference between  $T_C(\infty)$  and  $T_C^{\text{bulk}}$  for all three types of films. As can be seen in the Table II, however, even for  $l = 20$ ,  $\lambda'$  is not close to the expected large  $l$  value,  $1/\nu^{3d}$ . To elucidate further the evolution from  $2d$ - to  $3d$ -like behaviour we rearrange the power law of eqn. (7) and define

$$\lambda_{\text{eff}}(l_i) = -\log \left( \frac{T_C(\infty) - T_C(l_i)}{T_C(\infty) - T_C(l_{i-1})} \right) / \log \left( \frac{l_i}{l_{i-1}} \right), \quad (9)$$

and tabulate  $\lambda_{\text{eff}}(l_i)$  with  $l_i$  for both our Monte Carlo simulations ( $l_i \in \{4, 6, 8, 10, 15, 20\}$ ) and mean-field calculations ( $l_i$  ranging from 4 to 20 layers) in Table II. The  $\lambda_{\text{eff}}$ 's should converge to asymptotic shift

exponents  $1/\nu^{3d}$  when  $l$  tends to infinity. A linear least squares fit between  $\lambda_{\text{eff}}(l_i)$  and  $1/l_i$  enables us to obtain  $\lambda_{\text{eff}}(\infty)$  which is also given in the Table. (The mean-field values of  $\lambda_{\text{eff}}(\infty)$  for all structures all have values of 2 since the mean-field  $\nu$  is well-known to be  $1/2$ .) For the Monte Carlo simulations' results, it is gratifying to find  $\lambda_{\text{eff}}(\infty)$  to be close to  $1/\nu^{3d}$  which we obtain from our separate bulk Monte Carlo simulations. This gives good support to the contention of universality and the asymptotic behaviour contained in eqn. (7,8).

### C. Critical Exponents

Referring to equations (3), we notice that the critical exponents can be extracted from plots of  $\log m$  and  $\log \chi$ , as well as  $\log \frac{dU_L}{d\beta}$ , against  $\log L$  at  $T_C$ , provided that linear relations are found. This is actually the first test of the validity of our single correlation length,  $\xi$ , assumption. Results from our simulations, at  $T_C$ , indeed show very good linear relationships between  $\log m$ ,  $\log \chi$  and  $\log \frac{dU_L}{d\beta}$  with  $\log L$  for all our thin-films' thicknesses and structures. We note here that  $\frac{dU_L}{d\beta} \propto L^{1/\nu}$ . An example is shown in Fig. 4 which presents very good linear fits for 10-layered sc films. Now, the exponents  $\beta/\nu$ ,  $(\gamma/\nu)'$ , and  $1/\nu$  can be extracted from the slopes of the linear least square fits. They are listed in Table I. For the second test, we perform the summation of the computed exponents  $\left(\frac{\gamma}{\nu}\right)' + 2\frac{\beta}{\nu}$ . We have found that, in each case, this sum has a value of 2 within error bars as shown in Fig. 5. According to eqn. (4), this passes the second test for the assumption of a single  $\xi$  being sufficient to describe the critical behaviour of the thin-films. For the last test, we consider the scaling functions in eqn. (3). We calculate these scaling functions for the 10-layered sc films with  $L = 10, 20, 40, 60, 80, 100, 150$  and  $200$  using the exponents extracted from  $L = 64$  to  $128$ . The results are shown in Fig 6a,b. For large enough  $L$  ( $L = 60$  to  $200$ ), excellent data collapses occur. This confirms that our critical exponents are perfectly reliable. However, in the same figures, for small  $L$  (around  $L = 10$  and  $20$ ), data collapsing is not found. This is what we must expect since eqn. (3) originated from eqn. (A6,A7) (in appendix A) under the condition  $l \ll L$ . A collapse of scaling functions should not be observed if  $L$  approaches  $l$ . For comparison, we also present the scaling functions for these 10-layered sc films using the  $2d$  monolayer critical exponents in Fig 6c,d. We can see that the data collapses are not quite as good. This also confirms the reliability of our results.

Since our results pass all of the three tests above, it can be understood that the single  $\xi$  assumption is valid and eqn. (3) is very useful for extracting critical exponents from film systems at  $T_C$ . However, it is unfortunate that we cannot extract the  $\gamma/\nu$  out of  $(\gamma/\nu)'$  from our results. This means that we cannot investigate the dimension  $d$  as a function of thickness. Nevertheless, we find that the exponents  $(\gamma/\nu)'$  and  $\beta/\nu$ , for  $l = 1$  up to  $l = 20$  films, are quite close to their  $2d$  values as shown in Table I and Fig. 5. In particular, for thin-films ( $l \leq 8$ ), the exponent values seem to be almost identical with the  $2d$  results. On the other hand, for thicker films ( $l \geq 10$ ), a weak dependence of the exponents on  $l$  is found. This is somewhat reasonable since, in the critical region, although the correlation length  $\xi$  is  $2d$ -like in the sense that it can expand freely only in the  $xy$  plane, it is still a function of thickness. Suppose that at a reduced temperature  $t$  close to zero, any film has an in-plane correlation length  $\xi_{\parallel}$ . Then, the total magnitude of the correlation length  $\xi \approx \sqrt{(\xi_{\parallel})^2 + l^2}$  for different thickness  $l$  will also be different. The thicker the film, the more different from  $2d$  and the closer to  $3d$  it will be. However, thick films are beyond the scope of this study and we find that, for thin-films with thickness around 8 layers and thinner, the exponents are very close to the  $2d$  values. Thus, we feel that it is quite safe to conclude that thin-films belong to the  $2d$  class. In addition, our results show that, at a good level of agreement, the critical exponents from all structures represent the same universality class.

Finally, we compare our results for the exponent  $\beta$  with those available from an experiment with Ni films [3]. As shown in Fig. 7, the experimental results are close to ours only for films thinner than 4 layers. This is not surprising because the anisotropic Heisenberg magnet becomes Ising-like only for very thin-films. However, instead of a sharp dimensional crossover of  $\beta$  at around 5 to 8 layers [3], we found a trend which suggests that a dimensional crossover from  $2d$ - to  $3d$ -Ising should occur for much thicker films.

This is perhaps indicated by the slight increase of  $\beta/\nu$  towards its bulk value from  $l = 10$  onwards. This issue may also be partly answered in that the dimensional crossover of  $\beta$  in [3] may really be a transition from  $2d$ -Ising to  $3d$ -Heisenberg instead of from  $2d$ - to  $3d$ -Ising in our study. So, a direct comparison may not be allowed. Nevertheless, although Ising and Heisenberg films may be quantitatively different, they should qualitatively share same characteristics since, in the critical region, the divergence of  $\xi$  in both models is  $2d$ -like. So, it is strange that  $\beta$  in [3] should change its value so abruptly with very few layers. To find more answers, we consider [12] (Schilbe et al, 1996) which claimed ‘the author of [3] neglected the dependence of the (effective) critical exponents away from the critical point on the reduced temperature in their evaluation of the experimental data’. In other words, the range of temperatures  $10^{-3} < t < 10^{-1}$  used for the power law fit in [3] may not belong to the asymptotic behaviour (critical region), and the fit may lead to somewhat dubious results. So, to investigate this closely, we follow [12] who defined

$$\beta_{\text{eff}} = \frac{\partial \log m}{\partial \log t}, \quad (10)$$

and study how this varies with  $t$  in thin-films.

From Monte Carlo simulations in sc Ising thin-films for temperatures below but close to  $T_C$ , results of  $\log m$  against  $\log t$  for  $L \times L \times 10$  sc films are shown in Fig. 8. The figure shows how, close to  $T_C$ , for each  $L$ , the correlation length  $\xi$  notices the finite size  $L$ , that is where the finite size effect becomes important. Roughly, depending on the value of  $\nu$  (see Table I),  $\xi \propto t^{-\nu}$  will realise its finite limit at a temperature around  $\log t = -\frac{1}{\nu} \log L$ . We have also plotted  $\beta_{\text{eff}}$  against  $\log t$  for  $100 \times 100 \times l$  films in Fig. 9. It is found that the pattern of the  $\beta_{\text{eff}}$  curves is in agreement with the rough investigations in [12]. Since  $L = 100$  is used in our calculation, the  $\beta_{\text{eff}}$  are reliable (with minimum finite size effect) only down to  $\log t \simeq -2$ . However, this range of  $\log t$  does cover most of the range  $-3 < \log t < -1$  used in the power law fit in [3], and shows a quite interesting phenomenon. It appears that this range of temperature is not in the critical region because  $\beta_{\text{eff}}$  for each film is not constant, but peaks at a certain temperature. Outside the critical region, the correlation length grows as we increase the temperature towards  $T_C$ . As long as  $\xi$  is smaller than the film thickness, the film tries to behave as the  $3d$  bulk system and  $\beta$  grows somewhat towards the bulk value  $\beta^{3d} \approx 0.3258$  [21]. However, at some temperature  $\xi$  becomes comparable with the film thickness and is only allowed to expand in the in-plane direction, that is  $2d$  behaviour. Thus,  $\beta$  changes its trend and the resulting decrease results in a peak. We can also notice that the thicker the film, the closer the peak can grow towards the bulk value. Of course, if one tries to perform the power law fit in this range of temperature, a sudden change of  $\beta_{\text{eff}}$  will be observed.

We may conclude that the range  $-3 < \log t < -1$  used for the power law fit in [3] is outside the critical region and the power law fit should not work well. On the other hand, it must be emphasised that our exponents are extracted at the critical temperature by means of finite size scaling. Our exponents are the real critical exponents. This explains why the behaviour of  $\beta$  in [3] should not relate to our results.

#### IV. CONCLUSION

We have studied the magnetic behaviour of Ising thin-films in sc, bcc, and fcc structures using extensive Monte Carlo simulations. We have found the dimensional crossover of both the magnetisation  $m$  and the magnetic susceptibility  $\chi$  from  $2d$ - to  $3d$ -like with increasing film thickness. The layer-components of  $m$  and  $\chi$  have also been presented. The surface layers are found to have the lowest magnitudes whilst the innermost layers have the highest, a trend which is derived from the free boundary at the surface. (This behaviour is also found in our mean-field study.) We track how the films’ critical temperatures,  $T_C$ , evolve from  $2d$  to  $3d$  values with increasing film thickness. Results for square monolayers agree well with the exact Ising  $2d$   $T_C$  and our bulk  $3d$  results are also in good agreement with earlier studies in the literature. We are also able to fit our calculated  $T_C$ ’s for films of varying thickness,  $l$ , involving 3 parameters (shift exponents). This expression could be examined in the limit of infinitely thick films and the limit agrees

very well with that calculated directly from  $3d$  simulations. This fitting expression could also be used on the mean-field calculations.

We examine the critical regime of these systems in detail and extract critical exponents. For this purpose we develop a finite size scaling method for films. It is based on one assumption that a single correlation length  $\xi = \xi(l)$  is sufficient to describe the critical behaviour of Ising films. The validity of this assumption is successfully verified. From our results we find a very weak variation of the critical exponents with respect to  $l$ , the film thickness. For thin-films ( $l \leq 8$ ) the exponents are essentially the same as  $2d$  and from this it can be implied that thin-films fall into the  $2d$  class. For thicker films, however, ( $l \geq 10$ ) a weak  $l$  dependence is noticeable because  $l$  is thick enough for the correlation length to distinguish the geometry of the films from that of a simple  $2d$  lattice. As an example we present figures of the scaling functions for 10-layered sc films which are constructed by using both their own 10-layer critical exponents and also the well-known  $2d$  exponents. For large enough  $L$  (layer extent) we find good collapsing ( $L$ -independence) for the thickness-specific exponents which underscores the accuracy of our results. This collapse degenerates for  $L \rightarrow l$  which confirms that our finite size scaling analysis is valid only for  $L \gg l$ . When we use the  $2d$  critical exponents in the scaling functions a slightly poorer data collapse is found which points to the real disparity between thin-films and  $2d$  exponents.

In comparison with the experimental results described in [3] our results for the thinner films bear up well. A direct comparison, however, is not possible. This is because the experimental data from nickel films on a tungsten substrate can be interpreted to show a transition from  $2d$ -Ising to  $3d$ -Heisenberg rather than from  $2d$ -Ising to  $3d$ -Ising which is the only possibility for the model we have studied here. There is also the issue that the experimental data used to make a power law fit are taken from temperatures that are outside the critical regime.

*Acknowledgements* We acknowledge the use of computer resources provided by the Centre for Scientific Computing at the University of Warwick. One of us (Y. Laosiritaworn) would like to thank The Institute for The Promotion of Teaching Science and Technology (Thailand) for financial support (under DPST project) on his study.

## APPENDIX A: FINITE SIZE SCALING

We assume that the films' extent shows up when the correlation length growing along the  $z$  direction ( $\xi_z$ ) is about the same size as  $l$ , but  $\xi_x$  and  $\xi_y$ , the in-plane  $x$  and  $y$  correlation lengths, are still smaller than  $L$  and approach  $L$  when  $T \rightarrow T_C$ . So, for a film in the critical region, we propose a hypothesis that a single  $\xi$  is enough to describe the critical behaviour i.e.  $\xi_x = \xi_y = \xi$  with  $\xi_z = l$  as a constant. This implies  $\xi = \xi(l)$ . From this we modify a technique described by Binder and Wang [33]. The aim is to find out how thermodynamical properties such as  $m$  and  $\chi$  scale with  $L$  in a finite size lattice in the critical region where the film thickness  $l$  is a constant.

Consider the susceptibility

$$k_B T \chi = \frac{1}{L_x L_y L_z} \sum_{x_1=1}^{L_x} \sum_{y_1=1}^{L_y} \sum_{z_1=1}^{L_z} \sum_{x_2=1}^{L_x} \sum_{y_2=1}^{L_y} \sum_{z_2=1}^{L_z} \langle m(x_1, y_1, z_1) m(x_2, y_2, z_2) \rangle - \langle m \rangle^2, \quad (\text{A1})$$

where we set the lattice spacing as 1. We use periodic boundary conditions along the  $x$  and  $y$  directions. Changing the index  $z_2$  to  $z_1 + z$  under a condition that  $L_x$  and  $L_y \gg 1$ , we can write

$$k_B T \chi \simeq \frac{1}{L_z} \int_0^{L_x} dx \int_0^{L_y} dy \sum_{z_1=1}^{L_z} \sum_{z=1-z_1}^{L_z-z_1} \langle m(0, 0, z_1) m(x, y, z_1 + z) \rangle - \langle m \rangle^2. \quad (\text{A2})$$

Next, suppose that the two-point correlation function for an isotropically shaped system at  $T_C$  takes the form [34]

$$G_c^{(2)}(r, T_C) \equiv \langle m(0) m(r) \rangle - \langle m \rangle^2 \Big|_{T_C} \sim \frac{1}{r^{d-2+\eta}} \sim (x^2 + y^2 + z^2)^{-(d-2+\eta)/2} \quad (\text{A3})$$



(where  $r = |\vec{r}_1 - \vec{r}_2|$ ,  $d$  is the dimension of the system, and  $\eta$  is a critical exponent) and that this form is also valid for anisotropically shaped systems like films, we rewrite the susceptibility

$$k_B T_C \chi(T_C) \sim \frac{(L_x L_y)^{1-(d-2+\eta)/2}}{L_z} \int_0^1 dx' \int_0^1 dy' \sum_{z_1=1}^{L_z} \sum_{z=1-z_1}^{L_z-z_1} \left( \frac{L_x x'^2}{L_y} + \frac{L_y y'^2}{L_x} + \frac{z^2}{L_x L_y} \right)^{-(d-2+\eta)/2}, \quad (\text{A4})$$

where we have scaled the variables  $x \rightarrow L_x x'$  and  $y \rightarrow L_y y'$ . In the thin-film structure, we set  $L_x = L_y = L$  and  $L_z = l$ , so that

$$k_B T_C \chi(T_C) \sim \frac{(L^2)^{1-(d-2+\eta)/2}}{l} \int_0^1 dx' \int_0^1 dy' \sum_{z_1=1}^l \sum_{z=1-z_1}^{l-z_1} \left( x'^2 + y'^2 + \frac{z^2}{L^2} \right)^{-(d-2+\eta)/2}. \quad (\text{A5})$$

As  $z \in [1-l, l-1]$  and if we choose  $l \ll L$ ,  $\frac{z^2}{L^2} \ll 1$ , this yields  $\sum_{z_1=1}^l \sum_{z=1-z_1}^{l-z_1} (x'^2 + y'^2 + \frac{z^2}{L^2}) \approx l^2 (x'^2 + y'^2)$ . So the susceptibility becomes

$$\begin{aligned} k_B T_C \chi(T_C) &\sim l (L^2)^{1-\frac{d-2+\eta}{2}} \int_0^1 dx' \int_0^1 dy' (x'^2 + y'^2)^{-(d-2+\eta)/2} \\ &\propto L^{\gamma/\nu+2-d} l \propto L^{(\gamma/\nu)',} \end{aligned} \quad (\text{A6})$$

where the scaling relation  $\gamma/\nu = 2-\eta$  (e.g. [29]) has been used. Note that for a particular thin-film system,  $l$  is a constant so the only variable in the function is  $L$ . Consequently, in thin-films, if  $l \ll L$ ,  $\chi$  scales with  $L$  in the same way as isotropic-shaped systems, but with a different exponent  $(\gamma/\nu)' \equiv \gamma/\nu + 2 - d$ . For  $\langle m \rangle_{T_C}$ , we may assume that it is of the same order as the root mean square magnetisation  $\langle m^2 \rangle_{T_C}^{1/2}$ . So,

$$\begin{aligned} \langle m \rangle_{T_C} &\propto \langle m^2 \rangle_{T_C}^{1/2} = \left[ \frac{k_B T_C \chi(T_C)}{L^2 l} \right]^{1/2}, \\ &\propto L^{-\beta/\nu}, \end{aligned} \quad (\text{A7})$$

where again we have used  $\gamma/(2\nu) - d/2 = -\beta/\nu$  [29]. Note that since  $\xi = \xi(l)$  in our hypothesis is a function of thickness  $l$ , every exponent calculated in this way will also be a function of thickness.

## APPENDIX B: MEAN-FIELD APPROXIMATION

In a mean-field study of thin-films, the average Weiss field is layer-dependent. We write down the expression for the free energy for an  $l$ -layered films and obtain the equations of state from its minimisation with respect to the layer-resolved magnetisations  $m_k$  ( $k$  is a layer index). The  $l$ -coupled equations are solved numerically to extract the equilibrium magnetisations  $m_k$ . The magnetisation per site in the  $k^{\text{th}}$  layer is given as  $m_k = P_{k,\uparrow} - P_{k,\downarrow}$  where  $P_{k,(\uparrow,\downarrow)}$  is the probability of a site being occupied by an up (down) spin. Including the interaction with an external field ( $-h \sum_i S_i$ ) the interaction energy  $U$  is the sum over all layers ( $k = 1, \dots, l$ ) of terms  $E_k$  which are written as

$$E_k = -\frac{N_{\parallel}}{2} \left\{ Z_0 J_{kk} m_k^2 + Z_1 J_{k,k+1} m_k m_{k+1} (1 - \delta_{k,l}) + Z_1 J_{k,k-1} m_k m_{k-1} (1 - \delta_{k,1}) + 2h m_k \right\}, \quad (\text{B1})$$

where  $Z_0$  and  $Z_1$  are the number of nearest neighbors to a lattice site in the same layer and one of its adjacent layers, and  $N_{\parallel}$  is the number of sites in a layer. The free boundary condition necessitates the presence of the factors  $1 - \delta_{k,1}$  and  $1 - \delta_{k,l}$  in the equation. Similarly the entropy  $S$  can be written as  $S = \sum_{k=1}^l S_k$  where

$$\begin{aligned} S_k &= -k_B N_{\parallel} [P_{k,\uparrow} \ln P_{k,\uparrow} + (1 - P_{k,\uparrow}) \ln(1 - P_{k,\uparrow})] \\ &= -k_B N_{\parallel} \left[ \frac{1 + m_k}{2} \ln \frac{1 + m_k}{2} + \frac{1 - m_k}{2} \ln \frac{1 - m_k}{2} \right]. \end{aligned} \quad (\text{B2})$$

Thus, by minimising the free energy  $F = U - TS$  with respect to  $m_k$  i.e.  $\frac{\partial F}{\partial m_k} = 0$ , we obtain the equilibrium magnetisation in layer  $k$  by solving the following  $l$ -coupled equations for  $l$ -layered films

$$\begin{aligned} & -(Z_0 J_{1,1} m_1 + Z_1 J_{1,2} m_2 + h) + \frac{k_B T}{2} \ln \left[ \frac{1 + m_1}{1 - m_1} \right] = 0, \\ & -(Z_0 J_{k,k} m_k + Z_1 J_{k,k+1} m_{k+1} + Z_1 J_{k,k-1} m_{k-1} + h) + \frac{k_B T}{2} \ln \left[ \frac{1 + m_k}{1 - m_k} \right] = 0, \quad k = 2, \dots, l-1 \\ & -(Z_0 J_{l,l} m_l + Z_1 J_{l,l-1} m_{l-1} + h) + \frac{k_B T}{2} \ln \left[ \frac{1 + m_l}{1 - m_l} \right] = 0. \end{aligned} \quad (\text{B3})$$

$T_C$  can also be extracted from eqn. (B3) for zero external field. Close to  $T_C$ , the  $\{m_i\}$  are small and  $\ln \frac{1+m_k}{1-m_k} \approx 2m_k$  and  $T_C$  can be extracted by finding the temperature for which the set of equations  $\mathbf{A}\mathbf{m} = \mathbf{0}$ , where  $\mathbf{A}$  is a  $l \times l$  matrix with elements

$$A_{ij} = (k_B T - Z_0 J_{i,j}) \delta_{i,j} - Z_1 J_{i,j} \{ (1 - \delta_{i,1}) \delta_{i,j-1} + (1 - \delta_{i,l}) \delta_{i,j+1} \}, \quad (\text{B4})$$

and  $\mathbf{m}$  is a  $l \times 1$  column matrix,  $\{m_1, \dots, m_l\}$ , is satisfied.

- 
- [1] L.M. Falicov, D.T. Pierce, S.D. Bader, R. Gronsky, K.B. Hathaway, H.J. Hopster, D.N. Lambeth, S.S.P. Parkin, G. Prinz, M. Salamon, I.K. Schuller, and R.H. Victora, *J. Mater. Res.* **5**, 1299 (1990).
  - [2] M.T. Johnson, P.J.H. Bloemen, F.J.A. den Broeder, and J.J. de Vries, *Rep. Prog. Phys.* **59**, 1409 (1996).
  - [3] Y. Li and K. Baberschke, *Phys. Rev. Lett.* **68**, 1208 (1992).
  - [4] K. Binder and P.C. Hohenberg, *Phys. Rev. B* **9**, 2194 (1974).
  - [5] M. Bander and D.L. Mills, *Phys. Rev. B* **38**, 12015 (1998).
  - [6] H.J. Elmers, J. Hauschild, H. Höche, U. Gradmann, H. Bethge, D. Heuer and U. Köhler, *Phys. Rev. Lett.* **73**, 898 (1994).
  - [7] G.A.T. Allan, *Phys. Rev. B* **1**, 352 (1970).
  - [8] T.W. Capehart and M.E. Fisher, *Phys. Rev. B* **13**, 5021 (1976).
  - [9] D. O'Connor and C.R. Stephens, *Phys. Rev. Lett.* **72**, 506 (1994).
  - [10] D.L. Lin, H. Che and Y. Xia, *Phys. Rev. A* **46**, 1805 (1992);  
D.L. Lin, H. Che, W. Lai and T.F. George, *Phys. Rev. E* **49**, 2155 (1994);  
Y. Song, Y. Chen, J. Luo and D. Xian, *Phys. Lett. A* **221**, 124 (1996);  
J.T. Ou, F. Wang and D.L. Lin, *Phys. Rev. E* **56**, 2805 (1997).
  - [11] K. Binder, *Thin Solid Films* **20**, 367 (1974).
  - [12] P. Schilbe, S. Siebentritt, K.H. Rieder, *Phys. Lett. A* **216**, 20 (1996);  
P. Schilbe and K.H. Rieder, *Europhys. Lett.* **41**, 219 (1998);  
M.I. Marqués and J.A. Gonzalo, *Eur. Phys. J. B* **14**, 317 (2000);  
M.I. Marqués and J.A. Gonzalo, *Nanotechnology* **12**, 143 (2001).
  - [13] U. Wolff, *Phys. Rev. Lett.* **62**, 361 (1989).
  - [14] H. Müller-Krumbhaar and K. Binder, *J. Stat. Phys.* **8**, 1 (1973).
  - [15] P.C. Hohenberg and B.I. Halperin, *Rev. Mod. Phys.* **49**, 435 (1977).
  - [16] P. L'Ecuyer, in: *Handbook of Simulation*, ed. J. Banks (Wiley, 1998).
  - [17] K. Entacher. *A collection of selected pseudorandom number generators with linear structures*. Technical report, Dept. of Mathematics University of Salzburg (1997).
  - [18] P.D. Coddington, *Int. J. Mod. Phys. C* **5**, 547 (1994).
  - [19] K. Binder, *Z. Phys. B* **43**, 119 (1981).
  - [20] A.M. Ferrenberg and R.H. Swendsen, *Phys. Rev. Lett.* **61**, 2635 (1988).
  - [21] A.M. Ferrenberg and D.P. Landau, *Phys. Rev. B* **44**, 5081 (1991).

- [22] M.E.J. Newman and G.T. Barkema, *Monte Carlo Methods in Statistical Physics* (Oxford University Press, Oxford, 1999);
- [23] V. Privman, in: *Finite size scaling and Numerical Simulation of Statistical Systems*, ed. V. Privman (World Scientific, Singapore, 1990 reprinted 1998).
- [24] K. Binder, in: *Finite size scaling and numerical simulation of statistical systems*, ed. V. Privman (World Scientific, Singapore, 1990 reprinted 1998).
- [25] H.E. Stanley, *Introduction to Phase Transitions and Critical Phenomena* (Clarendon Press, Oxford , 1971).
- [26] M.E. Fisher, in: *Critical Phenomena, Proc. Int. School of Physics, "Enrico Fermi"*, Varenna, Italy, Course LI, ed. M.S. Green (Academic Press, New York, 1971).
- [27] M.N. Barber, in: *Phase Transitions and Critical Phenomena* Vol. 8, ed. C. Domb and J.L. Lebowitz (Academic Press Limited, London, 1983).
- [28] M.E. Fisher, Rev. Mod. Phys. **46**, 597 (1974).
- [29] M.E. Fisher, Phys. Rev. **180**, 594 (1969).
- [30] J. Adler, J. Phys. A **16**, 3585 (1983) *and references contained therein*.
- [31] W. Haubenreisser, W. Brodkorb, A. Corciovei and G. Costache, Phys. Status Solidi b **53**, 9 (1972) *and references contained therein*.
- [32] F. Huang, M.T. Kief, G.J. Mankey, and R.F. Willis, Phys. Rev. B **49**, 3962 (1994);  
S.Z. Wu, F.O. Schumann, G.J. Mankey, and R.F. Willis, J. Vac. Sci. Technol. **14**, 3189 (1996).
- [33] K. Binder and J.S. Wang, J. Stat. Phys. **55**, 87 (1989).
- [34] L.P. Kadanoff, Phys. **2**, 263 (1966).

	#layers	$T_C$		$\beta/\nu$	$\gamma/\nu + 2 - d$	$1/\nu$
		MC	MF			
	2D(Exact)	$\approx 2.269185$	4	0.125	1.75	1
sc	1	$2.2693 \pm 3 \times 10^{-4}$	4	$0.126 \pm 1 \times 10^{-3}$	$1.753 \pm 8 \times 10^{-3}$	$1.01 \pm 2 \times 10^{-2}$
	2	$3.2076 \pm 4 \times 10^{-4}$	5	$0.126 \pm 7 \times 10^{-3}$	$1.750 \pm 7 \times 10^{-3}$	$1.00 \pm 1 \times 10^{-2}$
	4	$3.8701 \pm 3 \times 10^{-4}$	5.61803	$0.125 \pm 2 \times 10^{-3}$	$1.730 \pm 1 \times 10^{-2}$	$1.00 \pm 2 \times 10^{-2}$
	6	$4.1179 \pm 3 \times 10^{-4}$	5.80194	$0.131 \pm 2 \times 10^{-3}$	$1.740 \pm 1 \times 10^{-2}$	$1.02 \pm 2 \times 10^{-2}$
	8	$4.2409 \pm 2 \times 10^{-4}$	5.87939	$0.141 \pm 2 \times 10^{-3}$	$1.744 \pm 7 \times 10^{-3}$	$1.03 \pm 1 \times 10^{-2}$
	10	$4.3117 \pm 3 \times 10^{-4}$	5.91899	$0.144 \pm 2 \times 10^{-3}$	$1.720 \pm 1 \times 10^{-2}$	$1.00 \pm 3 \times 10^{-2}$
	15	$4.3996 \pm 4 \times 10^{-4}$	5.96157	$0.162 \pm 2 \times 10^{-3}$	$1.680 \pm 1 \times 10^{-2}$	$1.02 \pm 1 \times 10^{-2}$
	20	$4.4381 \pm 2 \times 10^{-4}$	5.97766	$0.166 \pm 3 \times 10^{-3}$	$1.660 \pm 2 \times 10^{-2}$	$1.03 \pm 1 \times 10^{-2}$
	Bulk	$4.5115 \pm 2 \times 10^{-4}$	6	$0.507 \pm 4 \times 10^{-3}$	$0.980 \pm 1 \times 10^{-2}$	$1.57 \pm 3 \times 10^{-2}$
	Bulk*	$4.5390 \pm 6 \times 10^{-3}$	$6.00200 \pm 2 \times 10^{-4}$	-	-	-
bcc	2	$2.2691 \pm 1 \times 10^{-4}$	4	$0.120 \pm 5 \times 10^{-3}$	$1.760 \pm 3 \times 10^{-2}$	$1.01 \pm 1 \times 10^{-2}$
	4	$4.2947 \pm 3 \times 10^{-4}$	6.47214	$0.124 \pm 5 \times 10^{-3}$	$1.760 \pm 4 \times 10^{-2}$	$1.00 \pm 1 \times 10^{-2}$
	6	$5.1023 \pm 4 \times 10^{-4}$	7.20775	$0.130 \pm 6 \times 10^{-3}$	$1.762 \pm 6 \times 10^{-3}$	$1.02 \pm 1 \times 10^{-2}$
	8	$5.5005 \pm 3 \times 10^{-4}$	7.51754	$0.131 \pm 1 \times 10^{-3}$	$1.752 \pm 7 \times 10^{-3}$	$1.02 \pm 1 \times 10^{-2}$
	10	$5.7287 \pm 2 \times 10^{-4}$	7.67594	$0.136 \pm 1 \times 10^{-3}$	$1.748 \pm 7 \times 10^{-3}$	$1.04 \pm 1 \times 10^{-2}$
	15	$6.0076 \pm 4 \times 10^{-4}$	7.84628	$0.153 \pm 2 \times 10^{-3}$	$1.730 \pm 1 \times 10^{-2}$	$1.06 \pm 1 \times 10^{-2}$
	20	$6.1300 \pm 3 \times 10^{-4}$	7.91065	$0.169 \pm 3 \times 10^{-3}$	$1.700 \pm 1 \times 10^{-2}$	$1.06 \pm 1 \times 10^{-2}$
	Bulk	$6.3557 \pm 1 \times 10^{-4}$	8	$0.505 \pm 3 \times 10^{-3}$	$1.001 \pm 4 \times 10^{-3}$	$1.60 \pm 1 \times 10^{-2}$
	Bulk*	$6.3890 \pm 3 \times 10^{-3}$	$8.03200 \pm 4 \times 10^{-3}$	-	-	-
fcc	1	$2.2690 \pm 2 \times 10^{-4}$	4	$0.124 \pm 3 \times 10^{-3}$	$1.740 \pm 2 \times 10^{-2}$	$1.00 \pm 2 \times 10^{-2}$
	2	$5.2416 \pm 6 \times 10^{-4}$	8	$0.126 \pm 3 \times 10^{-3}$	$1.751 \pm 6 \times 10^{-3}$	$0.99 \pm 1 \times 10^{-2}$
	4	$7.5702 \pm 3 \times 10^{-4}$	10.47210	$0.126 \pm 1 \times 10^{-3}$	$1.750 \pm 1 \times 10^{-2}$	$0.99 \pm 3 \times 10^{-2}$
	6	$8.4431 \pm 3 \times 10^{-4}$	11.20780	$0.128 \pm 1 \times 10^{-3}$	$1.751 \pm 4 \times 10^{-3}$	$1.01 \pm 1 \times 10^{-2}$
	8	$8.8679 \pm 7 \times 10^{-4}$	11.51750	$0.130 \pm 2 \times 10^{-3}$	$1.740 \pm 1 \times 10^{-2}$	$1.00 \pm 1 \times 10^{-2}$
	10	$9.1106 \pm 6 \times 10^{-4}$	11.67590	$0.138 \pm 3 \times 10^{-3}$	$1.730 \pm 1 \times 10^{-2}$	$1.00 \pm 2 \times 10^{-2}$
	15	$9.4057 \pm 3 \times 10^{-4}$	11.84630	$0.153 \pm 2 \times 10^{-3}$	$1.720 \pm 1 \times 10^{-2}$	$1.03 \pm 2 \times 10^{-2}$
	20	$9.5353 \pm 5 \times 10^{-4}$	11.91060	$0.173 \pm 3 \times 10^{-3}$	$1.710 \pm 1 \times 10^{-2}$	$1.07 \pm 2 \times 10^{-2}$
	Bulk	$9.7736 \pm 2 \times 10^{-4}$	12	$0.498 \pm 8 \times 10^{-3}$	$0.994 \pm 9 \times 10^{-3}$	$1.59 \pm 3 \times 10^{-2}$
	Bulk*	$9.8600 \pm 2 \times 10^{-2}$	$12.04500 \pm 6 \times 10^{-3}$	-	-	-

TABLE I: The critical temperatures determined by both Monte Carlo (MC) simulations and also mean-field (MF) calculations for Ising films. Bulk  $3d$  results are also given for comparison. Bulk\* refers to the  $T_C(\infty)$  parameter of the fitting expression of eqn. (8). Critical exponents are given which have been extracted from the MC simulations via a finite size scaling analysis. Since we can extract the ratio of exponents  $\gamma/\nu$  for the bulk  $3d$  system we give  $(\gamma/\nu)'$  as  $\gamma/\nu + 2 - 3$

	Structure	$T_C(\infty)$	$l_0$	$l'$	$\lambda'$	$\lambda(\infty) = 1/\nu^{3d}$
MC	sc	$4.539 \pm 6 \times 10^{-3}$	$1.010 \pm 2 \times 10^{-2}$	$-0.010 \pm 2 \times 10^{-2}$	$1.280 \pm 2 \times 10^{-2}$	$1.578 \pm 3 \times 10^{-3}$
	bcc	$6.389 \pm 3 \times 10^{-3}$	$1.933 \pm 7 \times 10^{-3}$	$0.746 \pm 7 \times 10^{-3}$	$1.380 \pm 6 \times 10^{-3}$	$1.620 \pm 1 \times 10^{-2}$
	fcc	$9.860 \pm 2 \times 10^{-2}$	$1.416 \pm 6 \times 10^{-3}$	$0.440 \pm 7 \times 10^{-3}$	$1.300 \pm 1 \times 10^{-2}$	$1.621 \pm 8 \times 10^{-3}$
MF	sc	$6.0020 \pm 2 \times 10^{-4}$	$1.117 \pm 3 \times 10^{-3}$	$-0.61 \pm 4 \times 10^{-2}$	$1.894 \pm 3 \times 10^{-3}$	$2.002 \pm 4 \times 10^{-3}$
	bcc	$8.0320 \pm 4 \times 10^{-3}$	$1.380 \pm 1 \times 10^{-3}$	$0.63 \pm 2 \times 10^{-2}$	$1.600 \pm 6 \times 10^{-2}$	$2.002 \pm 2 \times 10^{-3}$
	fcc	$12.0500 \pm 6 \times 10^{-3}$	$1.120 \pm 1 \times 10^{-2}$	$0.28 \pm 1 \times 10^{-2}$	$1.580 \pm 1 \times 10^{-2}$	$2.000 \pm 2 \times 10^{-3}$

TABLE II: Fitting parameters for Ising thin-films using eqn. (8). MC and MF stand for Monte Carlo and mean-field respectively.

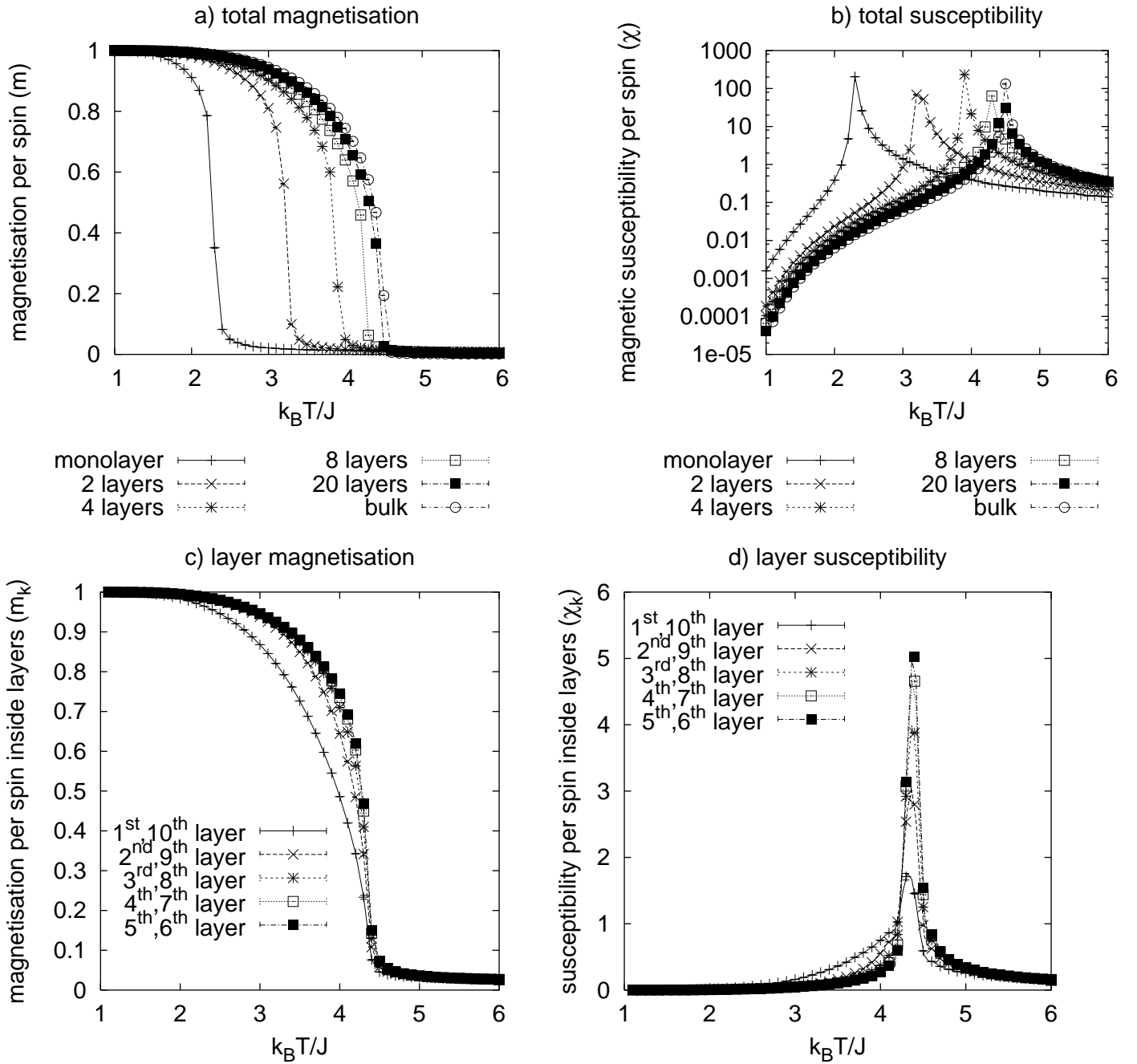


FIG. 1: The magnetic properties of Ising sc thin-films from Monte Carlo (MC) simulations. (a) and (b) show a dimensional crossover of  $m$  and  $\chi$  respectively from 2d- to bulk-like for  $128 \times 128 \times l$  spins ( $l$  is the number of layers in the film and  $l = 128$  represents the bulk system). (c) and (d) show the layer-dependence of  $m_k$  and  $\chi_k$ , where  $k$  is a layer index, in  $128 \times 128 \times 10$  sc films. Owing to the isotropic exchange interaction and spatial symmetry, layers  $k$  and  $10 - k$  have the same properties. Lines are added as a viewing aid. The error bars are smaller than point size.

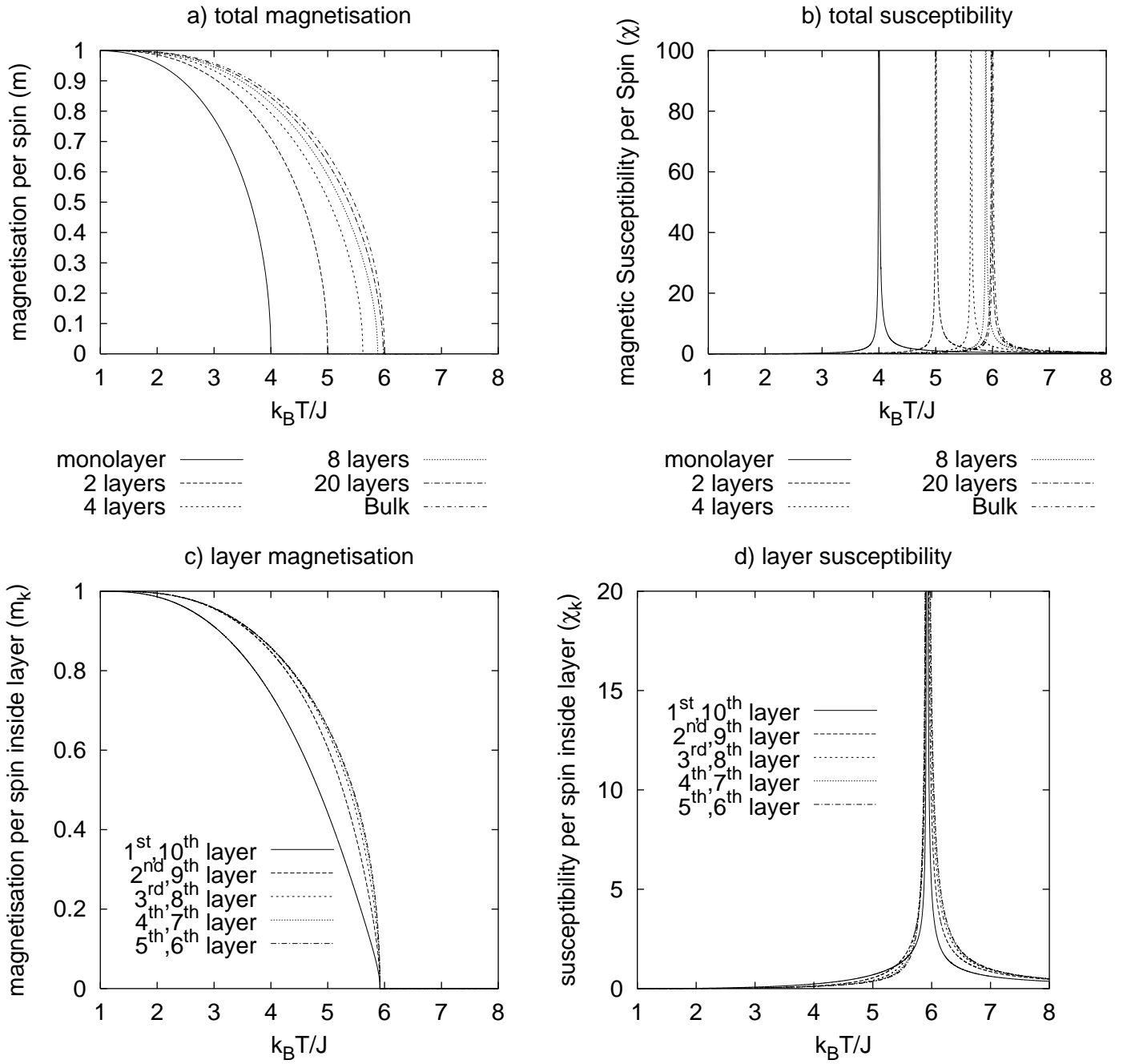


FIG. 2: The magnetic properties of Ising sc thin-films from mean-field calculations. As in Fig. 1, (a) and (b) show a crossover of  $m$  and  $\chi$  from the  $2d$  to the bulk limit ( $k_B T_C/J$  varies from 4 to 6). (c) and (d) show examples of the layer dependence of  $m_k$  and  $\chi_k$  for 10-layered sc films.

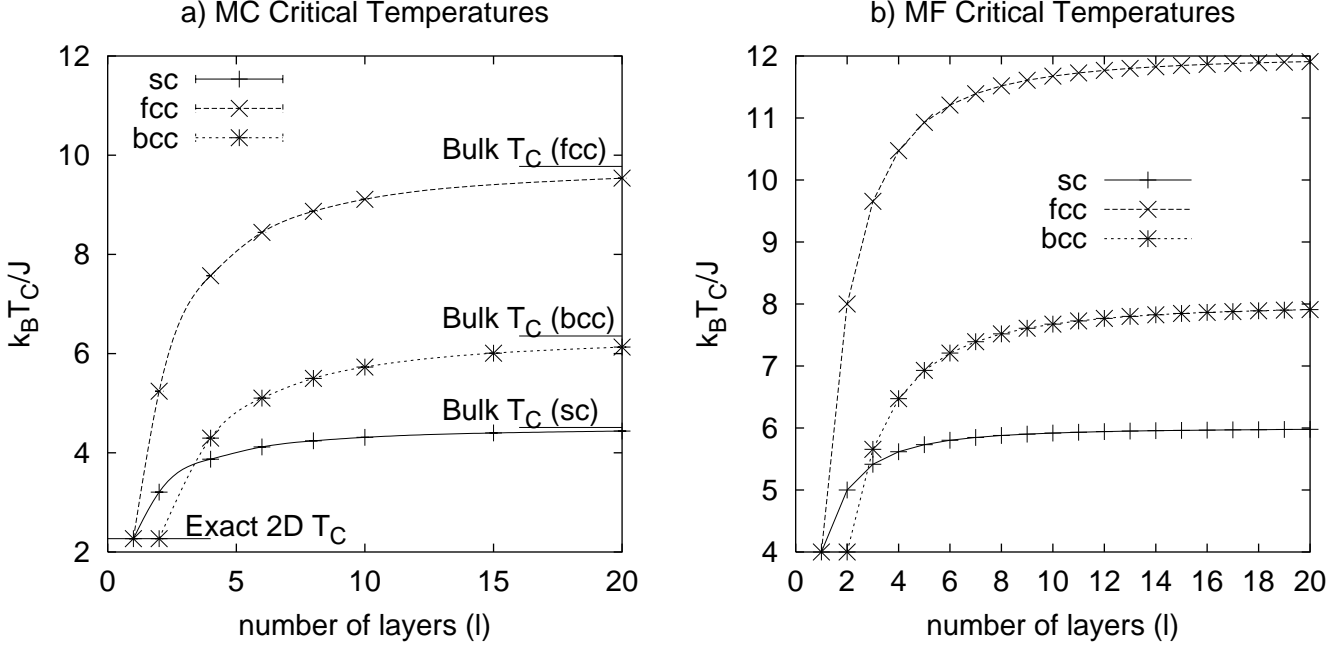


FIG. 3: The critical temperatures  $T_C$  as a function of thickness  $l$  extracted from (a) Monte Carlo simulations and (b) mean-field calculations. For mean-field, the values of  $k_B T_C / J$  are 4 for 2d and 6, 8 and 12 for bulk sc, bcc, and fcc respectively. Lines are added as a viewing aid. The error bars in (a) are smaller than point size.

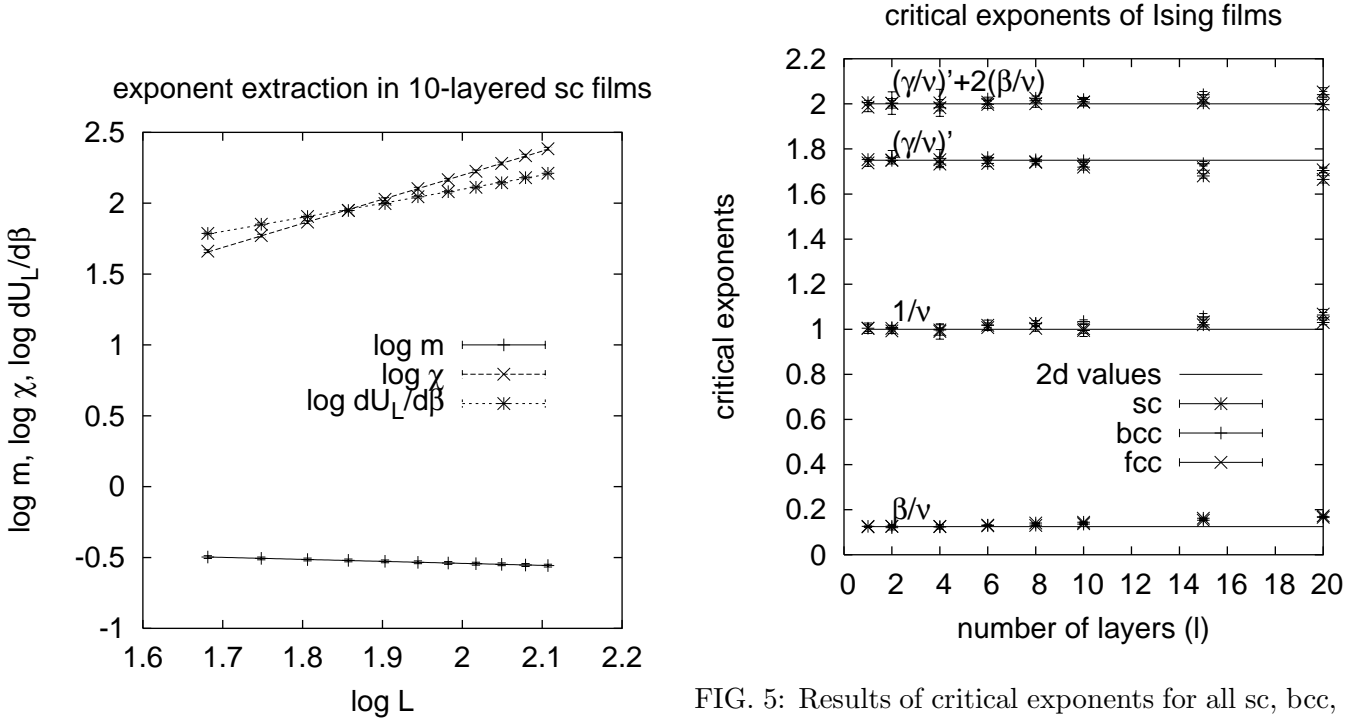


FIG. 4: An example of the extraction of critical exponents  $\beta, (\gamma/\nu)'$ , and  $1/\nu$  from the slope of a least-square-fit (see text) for 10-layered sc films. The apparent linear relation supports eqn. (3)

FIG. 5: Results of critical exponents for all sc, bcc, and fcc films. In all structures the exponents are very close to 2d values. Especially, for thin-films ( $l \leq 8$  approximately), the exponents are consistent with 2d results and suggest that thin-films belong to the 2d class. The summation  $(\gamma/\nu)' + 2\beta/\nu = 2$  supports our single correlation length  $\xi$  assumption.



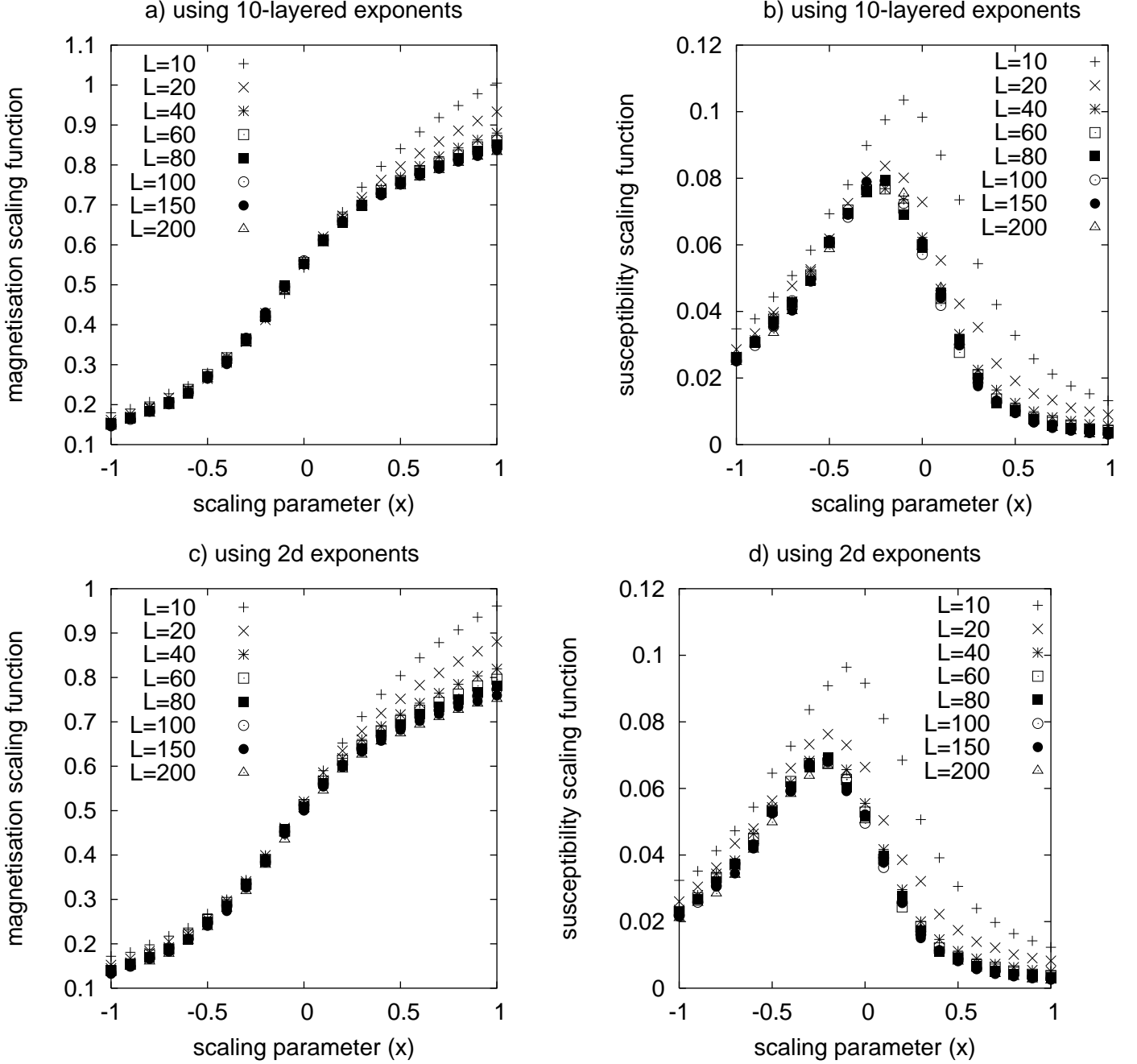


FIG. 6: The scaling functions for the magnetisation (a) and susceptibility (b) in 10 layered sc systems with  $L$  from 100 to 200 calculated by using those critical exponents extracted for 10-layered sc films with  $L$  ranging from 64 to 128. Analogous plots using 2d critical exponents are shown in (c) and (d). In (a) and (b), we find a good collapse of the data for all systems with  $L \geq 60$  including  $L = 150, 200$  which are bigger than those used in the exponent extraction. Note, however, that for  $L$  close to the thickness  $l = 10$ , the collapsing is not found since the assumption underpinning our finite size scaling relation (eqn. 3) rests on the condition  $L \gg l$ . In (c) and (d) we find a slightly worse collapsing than that in (a) and (b) - compare, for example, the collapsing around  $x = 1$  in (c) and (a). This confirms the weak  $l$  dependence of critical exponents and the deviation from the 2d values when the films thicken.

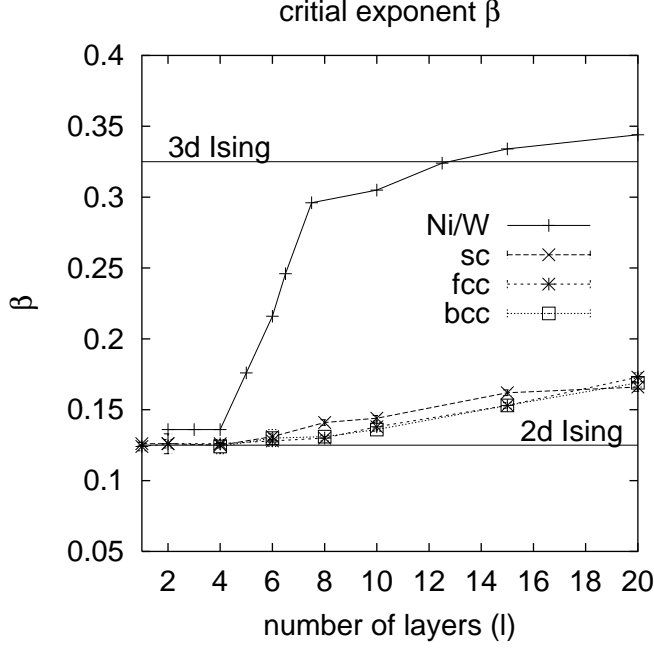


FIG. 7: Comparison of the critical exponent  $\beta$  extracted from experimental data for Ni(111)/W(110) in [3] and from Monte Carlo simulations of Ising thin-films.

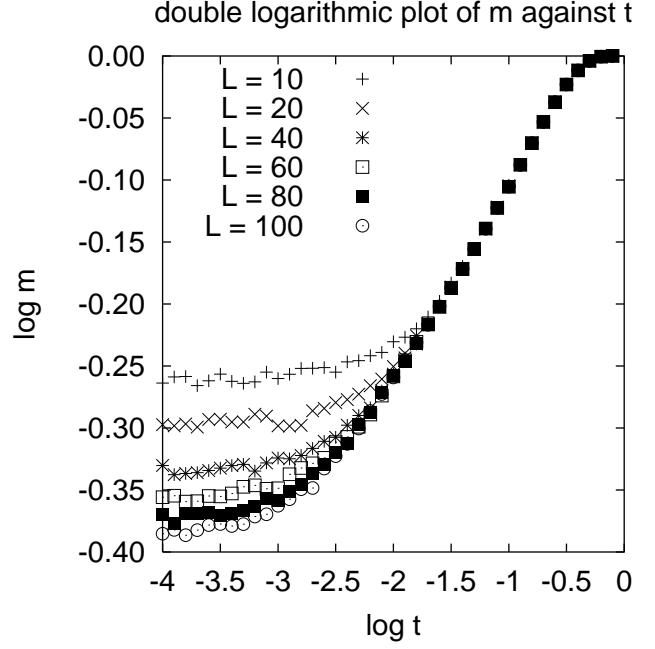


FIG. 8: Double logarithmic plot of  $m$  against  $t$ , the reduced temperature, for 4-layered Ising sc films. The finite size effect is evident once  $\xi$  becomes comparable to the size  $L$  of the layers of the films. Note the data is reliable down to  $\log t \approx -\frac{1}{\nu} \log L$

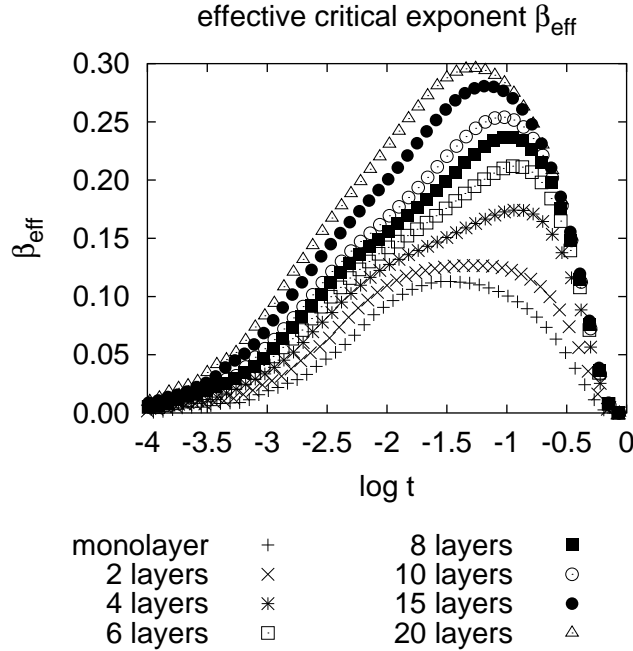


FIG. 9: The effective critical exponent  $\beta_{\text{eff}}$  extracted from  $100 \times 100 \times l$  sc Ising films where  $l$  is the number of layers. For  $l \geq 4$ , it is found that around  $\log t = -1$  to  $-1.5$ , the  $\beta_{\text{eff}}$  curves reach peaks and this indicates how a step-like function of  $\beta$  of the form described in [3] i.e. Fig. 7 is possible.